Received: 20 December 2019 | Revised: 6 February 2020 | Accepted: 6 February 2020

DOI: 10.1111/jace.17060

ORIGINAL ARTICLE

Journal of the American Ceramic Society

Thermodynamic assessment of $BaO–Ln_2O_3$ (Ln = La, Pr, Eu, Gd, Er) systems

Weiping Gong[1] | **Yanzhi Liu**[2] | **Yun Xie**[1] | **Zhenting Zhao**[1] | **Sergey V. Ushakov**[3] | **Alexandra Navrotsky**[3,4]

[1]Guangdong Provincial Key Laboratory of Electronic Functional Materials and Devices, Huizhou University, Huizhou, P. R. China

[2]Department of Chemical and Biomolecular Engineering, Clarkson University, Potsdam, NY, USA

[3]Peter A. Rock Thermochemistry Laboratory and NEAT ORU, University of California Davis, Davis, CA, USA

[4]School of Molecular Sciences and Center for Materials of the Universe, Arizona State University, Tempe, AZ, USA

Correspondence
Weiping Gong, Guangdong Provincial Key Laboratory of Electronic Functional Materials and Devices, Huizhou University, Huizhou 516001, Guangdong, P. R. China.
Email: gwp@hzu.edu.cn

Alexandra Navrotsky, Peter A. Rock Thermochemistry Laboratory and NEAT ORU, University of California Davis, Davis, CA 95616, USA.
Email: alexnav@asu.edu

Funding information
National Natural Science Foundation of China, Grant/Award Number: 21606053, 51171069, 51602121 and 51672100; National Science Foundation, Grant/Award Number: DMR 1835848; National Study Abroad Fund (China); International Science and Technology cooperation project of Guangdong Province, Grant/Award Number: 2019A050510049; Natural Science Foundation of Guangdong Province, Grant/Award Number: 2017A030310665

Abstract

Heat capacities and enthalpies of formation of $BaGd_2O_4$ were determined by high-temperature differential scanning calorimetry and high-temperature oxide melt solution calorimetry, respectively. Thermodynamic stability of $BaLn_2O_4$ compounds increases with decreasing Ln^{3+} ionic radius. Previously reported data on $BaNd_2O_4$ and $BaSm_2O_4$ corroborate this trend. Missing data for compounds in $BaO–Ln_2O_3$ (Ln = La, Pr, Eu, Er) systems were estimated from established relations, thermodynamic assessment was performed, and binary phase diagrams were calculated.

KEYWORDS

$BaLn_2O_4$, $BaO–Gd_2O_3$, enthalpy of formation, heat capacities, phase diagram

 © 2020 The American Ceramic Society

1 | INTRODUCTION

$BaLn_2O_4$ compounds (Ln = rare earth) crystallize in the $CaFe_2O_4$ structure type with *Pnma* space group. In this structure, Ln^{3+} adopts a triangular array resulting in geometrically frustrated magnetic and other interesting physical properties.[1–3] Studies on the $CaFe_2O_4$-type compounds reported a series of phenomena, such as noncollinear magnetic ground states, Jahn-Teller effects, Ising chains, magnetic chirality, and geometric magnetic frustration.[1–5]

$BaLn_2O_4$ were first reported by Lopato,[6] who successfully synthesized $BaLn_2O_4$ for Ln = La-Er and Y by calcination reaction between barium carbonate and lanthanide oxide. According to Lopato's work,[6] the melting temperature of $BaLn_2O_4$ increased when Ln going from La to Sm and then decreased in the series from Gd to Er The same pattern was observed in the yield of $BaLn_2O_4$ product with this synthesis route. Construction of reliable phase diagrams for BaO–Ln_2O_3 systems is critical for development and optimization of $BaLn_2O_4$ synthesis routes and predicting their stability in various environments.

Lopato[6] performed the only experimental study of the phase diagrams of the BaO–Ln_2O_3 systems. She studied the reactions of rare earth oxides with oxides of Mg, Ca, Sr, and Ba by differential thermal analysis (DTA) and by room-temperature X-ray diffraction (XRD) on samples quenched from 1273 to 2723 K. She reported a series of phase diagrams of the rare earth oxide-alkaline earth oxide systems, including the BaO–La_2O_3 and BaO–Sm_2O_3 systems. In the BaO–La_2O_3 system, $BaLa_2O_4$ was the only binary compound and was reported to be stable at room temperature. In the BaO–Sm_2O_3 system, a $Ba_3Sm_4O_9$ line compound was detected in addition to $BaSm_2O_4$, which was also stable at room temperature.[6] For both the BaO–La_2O_3 and BaO–Sm_2O_3 systems and for some SrO–Ln_2O_3 and CaO–Ln_2O_3 systems, the solid solutions X_{SS}, H_{SS}, A_{SS}, and B_{SS} were detected. They were related to the cubic *X*-form, hexagonal *H*-form and *A*-forms, or monoclinic *B*-form of Ln_2O_3 polymorphs. The limited solubility of Ln_2O_3 in BaO was ignored.[6]

Literature data on the thermodynamic properties of $BaLn_2O_4$ are scarce. Electromotive force methods (EMFs) were used by several researchers to derive temperature dependence of the Gibbs energies of formation of $BaLn_2O_4$ from BaO and Ln_2O_3, where Ln = Nd, Sm, Eu, Gd, Dy, Ho, and Er[7–10] All reports indicated that the compounds are thermodynamically stable with respect to oxides. However, there are significant discrepancies in reported values.[7–11] As shown in Figure 1 and Table 1, the Gibbs energy of formation and the enthalpy of formation of $BaSm_2O_4$ from the binary oxides determined by Xing et al[7] differ by a factor of two from those of Subasri and Sreedharan,[8] and even more from the results of Uspenskaya et al[9] and Vakhovskaya et al[10] Although the values of enthalpy of formation

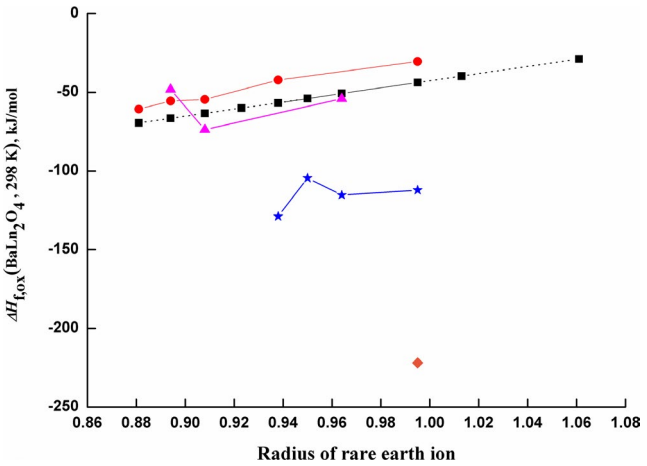

FIGURE 1 Enthalpies of formation of $BaLn_2O_4$ from the component oxides at 298 K. --■-- (black on line), values measured in this work; --■-- (black on dotted line), values predicted in this work on the relation of enthalpy of formation with the radius of rare earth ion; --●-- (red on line), values from Vakhovakaya et al[10]; - -▲-(purple on line), values from Uspenskaya et al[9]; --★-- (blue on line), values from Subarsi and Sreedharan[8]; ◆(orange dot), value from Xing et al[7]

reported by Uspenskaya et al[9] and Vakhovskaya et al[10] were close to each other and their Gibbs energy functions of $BaDy_2O_4$ and $BaHo_2O_4$ were identical, they reported different values for enthalpies of formation of $BaDy_2O_4$ and $BaHo_2O_4$. Surprisingly, these conflicting reports came from the same group in Moscow State University. Uspenskaya and Vakhovskaya coauthored the articles,[9,10] but they did not discuss this obvious discrepancy.

Recently, Gong et al[11,12] presented thermodynamic databases and phase diagrams of the BaO-Sm_2O_3 and BaO-Nd_2O_3 systems with new results for the $BaSm_2O_4$ and $BaNd_2O_4$ compounds—enthalpies of formation from oxides at 298 K and heat capacities in the temperature range 573-1073 K. The obtained enthalpies of formation of $BaSm_2O_4$[11] and $BaNd_2O_4$[12] are in the range of values reported by Uspenskaya et al[9] and Vakhovskaya et al,[10] and substantially less negative than those reported by Xing et al[7] and Subarsi and Sreedharan.[8] Thermodynamic assessment of the BaO–Sm_2O_3 system by Gong et al[11] reported incongruent melting of $BaSm_2O_4$ by the peritectic reaction $BaSm_2O_4 \leftrightarrow$ liquid + $Ba_3Sm_4O_9$, confirmed with DTA experiments. Congruent melting of $BaSm_2O_4$ was assumed in Lopato's earlier phase diagram.[6] For the BaO-Nd_2O_3 system, thermodynamic calculations reproduced the thermodynamic data of $BaNd_2O_4$ measured by Gong et al[12] and confirmed phase equilibria similar to those of the BaO–La_2O_3 system.[6]

Neither thermodynamic data on $BaLa_2O_4$ nor thermodynamic calculations on the BaO–La_2O_3 system have been reported. The phase diagram of the BaO–Gd_2O_3 system was reported to be similar to that of BaO–Sm_2O_3 system.[6] In this work, we present new thermodynamic data on the $BaGd_2O_4$ compound, estimate missing data for $BaLn_2O_4$ (Ln = La, Pr, Eu,

TABLE 1 Summary of the Gibbs energy functions of formation and the enthalpy of formation of $BaLn_2O_4$ from simple oxides in literature[7–12]

Compound	$\Delta G_{f,\,ox}$ (kJ/mol)	$\Delta H_{f,\,ox}$ (kJ/mol)	References
$BaNd_2O_4$	$-112.14 + 19.2 \times 10^{-3}T$	-112.1	8
	$-(30.4 \pm 8.6)+(10.3 \pm 7.0) \times 10^{-3}T$	-30.4 ± 8.6	10
	$-44.27 + 12.0 \times 10^{-3}T$	-44.27	12
$BaSm_2O_4$	$-221.9 + 0.1216T$	-221.9	7
	$-115.28 + 5.0 \times 10^{-3}T$	-115.3	8
	$-(53.2 \pm 8.1) + (27.2 \pm 6.8) \times 10^{-3}T$	-54.0 ± 3.0	9
		-51.09	11
$BaEu_2O_4$	$-104.50 + 6.2 \times 10^{-3}T$	-104.5	8
$BaGd_2O_4$	$-128.84 + 32.0 \times 10^{-3}T$	-128.8	8
	$-(42.2 \pm 6.5) + (12.8 \pm 5.1) \times 10^{-3}T$	-42.2 ± 6.5	10
$BaDy_2O_4$	$-(54.5 \pm 7.9) + (24.8 \pm 6.1) \times 10^{-3}T$	-73.7 ± 5.0	9
	$-(54.5 \pm 7.9) + (24.8 \pm 6.1) \times 10^{-3}T$	-54.5 ± 7.9	10
$BaHo_2O_4$	$-(55.5 \pm 8.4) + (24.9 \pm 7.0) \times 10^{-3}T$	-48.1 ± 7.1	9
	$-(55.5 \pm 8.4) + (24.9 \pm 7.0) \times 10^{-3}T$	-55.5 ± 8.4	10
$BaEr_2O_4$	$-(60.7.5 \pm 7.1) + (30.0 \pm 5.5) \times 10^{-3}T$	$-60.7.5 \pm 7.1$	10

Er), and use the Calculation of phase diagrams (CALPHAD) methodology to produce internally consistent thermodynamic databases for $BaO–Ln_2O_3$ (Ln = La, Pr, Eu, Gd, Er) systems.

2 | EXPERIMENTAL PROCEDURES

2.1 | Sample preparation and characterization

The samples were synthesized at UC Davis using solid-state reaction techniques. $BaCO_3$ (Fisher, 99.6 wt%), La_2O_3, and Gd_2O_3 (from Alfa Aesar, 99.9 wt%) were used to prepare $BaLa_2O_4$ and $BaGd_2O_4$, respectively. Starting mixtures were preheated at 1073 K for 12 hours to remove any moisture and then stored in a desiccator. About 2 g of each sample was prepared by first grinding $BaCO_3$ and Ln_2O_3 (Ln = La, Gd) with the appropriate molar ratio in an agate mortar. The mixtures were pressed into pellets and placed in Pt crucibles in a Deltech platform furnace held at 1088 K. The samples were heated to 1573 or 1673 K, held for 3 hours, and taken out of the furnace after cooling to 1088 K. Experiments were performed in air with heating and cooling rates of 10 K/min. The products were analyzed by XRD and synthesis was repeated with additional regrinding to obtain a single phase.

XRD analysis was performed with a Bruker D8 Advance X-ray diffractometer using a CuK_α radiation at 40 kV and 40 mA emission current using 15°-80° 2θ range, 0.02° step size, and scan speed of 0.25°/s. JADE 6.0 software was used for phase identification.

3 | CALORIMETRIC MEASUREMENTS

A Setaram LabSYS differential scanning calorimeter (DSC) was used to determine the heat capacities of $BaGd_2O_4$ from 573 to 1273 K. The measurements were performed by the continuous method in argon flow (20 mL/min) with a heating rate of 10 K/min using standard procedures, following the Standard Test Method for Determining Specific Heat Capacity by Differential Scanning Calorimetry (ASTM).[13] Three consecutive runs using an empty crucible, α-Al_2O_3 standard, and the sample were performed under identical experimental conditions. Samples were packed tightly into platinum crucibles to ensure good thermal contact leading to reproducibility of the heat capacity data. The measurements were repeated three times to achieve reliable data. DSC sensitivity calibration was performed with a α-Al_2O_3 standard using the heat capacity equation from the National Institute of Standards and Technology (NIST).[14]

The enthalpies of formation of $BaLa_2O_4$ and $BaGd_2O_4$ were determined by high-temperature oxide melt solution calorimetry, using standard procedures described in detail elsewhere.[15–17] The samples were loosely hand-pressed into pellets, 5-10 mg in weight, and dropped from room temperature into 20 g of molten oxide solvent ($3Na_2O{\cdot}4MoO_3$) in a platinum crucible inside the calorimeter chamber. Oxygen gas was flushed through calorimeter assembly at 40 mL/min and bubbled through the solvent at 4 mL/min to maintain an oxidizing environment, enhance the dissolution, and prevent local saturation of the melt. The calorimetric measurements on $BaGd_2O_4$ were carried out at 973 K and at 1073 K for $BaLa_2O_4$. The measured drop solution enthalpy ΔH_{ds} is a sum of the molar heat content of the sample

from 298 K to the calorimeter temperature (973 or 1073 K) and its enthalpy of solution in the solvent at calorimeter temperature. The calorimeter was calibrated using the heat content[14] of α-Al_2O_3 pellets dropped into an empty platinum crucible. The drop solution experiments were repeated at least eight times to achieve statistically reliable data with two standard deviations of ±(1-2)%. The previously measured drop solution enthalpies of BaO, La_2O_3, and Gd_2O_3, which were done by Navrotsky's group[17,18] under identical experimental conditions as those in the present work, were used in thermochemical cycles to calculate the enthalpy of formation of $BaLa_2O_4$ and $BaGd_2O_4$ from oxides. The accuracy of the enthalpy of formation obtained in this method is typically within the range of ±(1-5) kJ/mol.

4 | EXPERIMENTAL RESULTS

Figure 2 shows the XRD patterns of the $BaLa_2O_4$ and $BaGd_2O_4$ compounds quenched from 1673 and 1573 K. The obtained single-phase $BaGd_2O_4$ has $CaFe_2O_4$-type structure with primitive orthorhombic symmetry (space group *Pnma*). The refined lattice cell parameters are a = 10.486 Å, b = 12.261 Å, and c = 3.514 Å. A single phase of $BaLa_2O_4$ was not obtained despite multiple regrinding and heat treatment. Probably due to the evaporation of BaO at the higher temperature, large amounts of unreacted rare earth oxides were detected in the synthetic $BaLa_2O_4$; similar results were reported earlier for $BaNd_2O_4$.[12] Rietveld analysis of XRD patterns using JADE 6.0 software indicated 38 mol% residual La_2O_3 in $BaLa_2O_4$ synthesis compared with 15 mol% of Nd_2O_3 for $BaNd_2O_4$.[12] The refined lattice cell parameters of $BaLa_2O_4$ are a = 10.668 Å, b = 12.642 Å, and c = 3.704 Å, which are slightly larger than those of $BaGd_2O_4$ and $BaSm_2O_4$.[11] Synthesis procedure and the XRD results demonstrate that the yield of $BaLn_2O_4$ increases

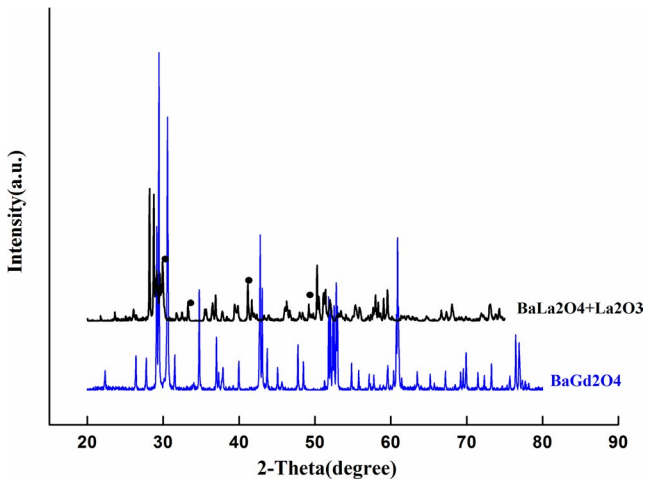

FIGURE 2 XRD patterns of the synthetic $BaLa_2O_4$ and $BaGd_2O_4$ compounds quenched from 1673 K and 1573 K. Peaks marked with ● are related to La_2O_3

from La to Gd, which is in agreement with the more exothermic enthalpy of formation from La to Gd, as shown below.

The enthalpy of formation ($\triangle H_{f,ox}$) of $BaGd_2O_4$ from oxides was calculated using the following thermochemical cycle:

$$BaGd_2O_4\ (s, 298\ K) \rightarrow Gd_2O_3\ (sn, 973\ K) + BaO\ (sn, 973\ K)\ \Delta H_1 \quad (1)$$

$$Gd_2O_3\ (s, 298\ K) \rightarrow Gd_2O_3\ (sn, 973\ K)\ \Delta H_2 \quad (2)$$

$$BaO\ (s, 298\ K) \rightarrow BaO\ (sn, 973\ K)\ \Delta H_3 \quad (3)$$

$$Gd_2O_3\ (s, 298\ K) + BaO\ (s, 298\ K) \rightarrow BaGd_2O_4\ (s, 298\ K)\ \Delta H_4 \quad (4)$$

where $\triangle H_1$, $\triangle H_2$, and $\triangle H_3$ are related to the enthalpy of drop solution of $BaGd_2O_4$, Gd_2O_3, and BaO, respectively. $\triangle H_4$ corresponds to $\triangle H_{f,ox}$ for $BaGd_2O_4$ at 298 K.

$$\Delta H_4 = \Delta H_2 + \Delta H_3 - \Delta H_1 \quad (5)$$

The measured drop solution enthalpy for $BaGd_2O_4$, reference values for BaO and Gd_2O_3,[17,18] and obtained $\triangle H_{f,ox}$ for $BaGd_2O_4$ are listed in Table 2. Previously reported values for $BaSm_2O_4$[11] and $BaNd_2O_4$[12] are included for comparison.

It can be seen that $BaGd_2O_4$ shows the largest exothermic enthalpy of formation. As shown in Figure 1, an approximately linear increase in the exothermic enthalpy formation of $BaLn_2O_4$ (Ln = Nd, Sm, and Gd) is observed in relation to the increasing radius of the rare earth ion. A similar correlation was observed by Vakhovakaya et al,[10] although they reported less negative values for formation enthalpies. On this basis, the formation enthalpy for $BaLa_2O_4$ was predicted to be –28.4 kJ/mol. The enthalpies of formation of the compounds $BaPr_2O_4$ (−39.6 kJ/mol), $BaEu_2O_4$ (−53.9 kJ/mol), and $BaEr_2O_4$ (−69.5 kJ/mol) were also predicted, the estimated error is less than 2%, which differed from the values of Vakhovakaya et al[10] The present study indicates that the thermodynamic stability of $BaLn_2O_4$ increases with Ln going from La to Er, in contrast with the Lopato[6] prediction of a stability decrease from Gd to Er The present values of the enthalpy formation of $BaLn_2O_4$ (Ln = La, Nd, Sm, and Gd) are substantially less exothermic than those reported by Xing et al[7] and Subarsi and Sreedharan.[8] We attribute the large discrepancies of Xing et al[7] and Subarsi and Sreedharan[8] to the use of $BaZrO_3|ZrO_2|BaF_2$ as the reference electrode in the temperature range 900-1150 K. Levitskii[19] demonstrated that reproducible electromotive force values for this electrode can be obtained only at temperatures above 1200 K.

The measured heat capacity versus temperature for $BaGd_2O_4$ is shown in Figure 3 as the mean of three runs. The estimated errors are always less than 3.5% and often less than 2%. Values from the Neumann-Kopp rule (NKR) calculation

TABLE 2 Determined enthalpy of drop solution of $BaGd_2O_4$ in $3NaO{\cdot}4MoO_3$ solvent at 973 K and the thermodynamic cycle used for calculation of enthalpy of formation of the compounds at 298 K from their constituent oxides, cubic Gd_2O_3 and rock salt BaO

	ΔH_{ds}, kJ/mol			
	T_0 = 973 K	T_0 = 1073 K	$\Delta H_{f,ox}$	References
BaO	−184.61 ± 3.21	−176.48 ± 3.48		12,17
Gd_2O_3	−144.34 ± 1.35			18
$BaGd_2O_4$	−272.32 ± 2.88		−56. 63 ± 4.52	This work[dr]
			−56.51	This work[cal]
$BaSm_2O_4$	−287.56 ± 3.64		−50.67 ± 5.63	11[dr]
			−51.09	11[cal]
$BaNd_2O_4$		−274.93 ± 3.02	−43.75 ± 4.68	12[dr]
			−44.27	12[cal]
$BaLa_2O_4$			−28.4	This work[pre]
$BaPr_2O_4$			−39.6	This work[pre]
$BaEu_2O_4$			−53.9	This work[pre]
$BaEr_2O_4$			−69.5	This work[pre]

Note: [dr]means, the values obtained from the high-temperature oxide melt solution calorimetry. [cal]means, the values calculated from the thermodynamic parameters optimized by CALPHAD. [pre]means, the values predicted from the general rule of the enthalpy of formation versus the radius of rare earth ion.

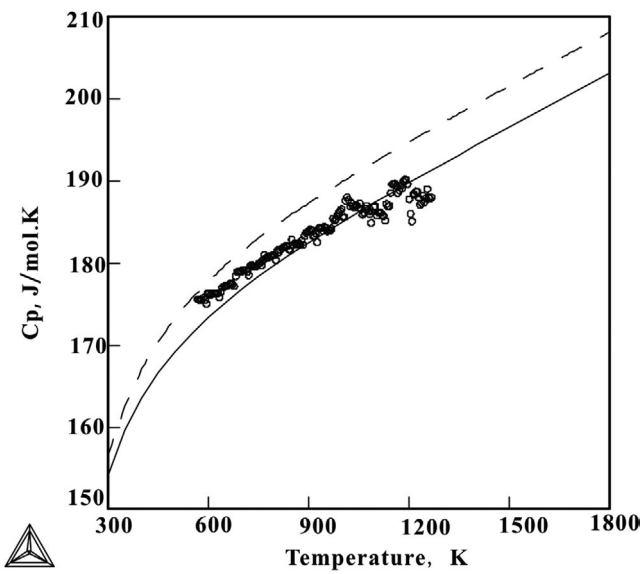

FIGURE 3 Measured heat capacities of $BaGd_2O_4$ in this work identified with the symbols ○. The solid and dot curves represent the Neumann-Kopp rule calculations on the $BaGd_2O_4$ and $BaLa_2O_4$, respectively

based on the data of BaO and Gd_2O_3 from references[11,20] are also shown for comparison. Heat capacities of $BaGd_2O_4$ follow the NKR calculation within experimental uncertainty, similar to earlier reported results for $BaNd_2O_4$.[12] The NKR calculation also agrees with the measured heat capacity of $BaSm_2O_4$ within 3%.[11] Thus, NKR is a valid approximation of the heat capacity for $BaGd_2O_4$ and can be accepted for uninvestigated $BaLn_2O_4$ using the corresponding oxide values. Measurements on $BaLa_2O_4$ were not performed in this work due to the large content of unreacted La_2O_3.

5 | THERMODYNAMIC MODELING AND CALCULATIONS

The CALPHAD method[21] was employed for thermodynamic assessment of BaO–Ln_2O_3 (Ln = La, Pr, Eu, Gd, Er) using literature data,[6] and new measurements for $BaGd_2O_4$.

The Gibbs energy function $G_i^{0,\varphi}(T) = G_i^{\varphi}(T) - H_i^{SER}$ for the pure binary component i (i = BaO, La_2O_3, Gd_2O_3) in phase φ was expressed by the following equation:

$$G_i^{0,\varphi}(T) = a + bT + cT\ln T + dT^2 + eT^{-1} + fT^3 + gT^7 + hT^{-9} \quad (6)$$

where H_i^{SER} is the molar enthalpy of the component i at 298 K and 101 325 Pa in its standard element reference (SER) state, and T is the absolute temperature. The last two terms in Equation (6) are used only outside the ranges of stability,[22] thus avoiding the possibility of a solid phase becoming stable at high temperatures or a liquid phase becoming stable at low temperature. In the present work, the Gibbs energy functions of pure La_2O_3 and Gd_2O_3 in liquid, X_{SS}, H_{SS}, A_{SS}, and B_{SS} phases were taken from the assessments of Zinkevich.[20] Those of BaO in liquid and rock salt structures as well as in the hypothetical metastable phases were taken from our previous assessment.[11]

The liquid, X_{SS}, H_{SS}, A_{SS}, B_{SS}, and BaO-based solid solution phases as well as the $BaLa_2O_4$ or $BaGd_2O_4$ and $Ba_3Gd_4O_9$ compounds were taken into account during the thermodynamic modeling and calculations on the BaO–La_2O_3 and BaO–Gd_2O_3 systems. As part of an ongoing program as well as for compatibility, the solution phases in the systems are thermodynamically described by the same substitutional solution model as in our previous work.[11,12] Thus,

the Gibbs energy for each solution phase was expressed by Redlich-Kister polynomials[23] as Equation (7).

$$\begin{aligned} G_{\mathrm{m}}^{\mathrm{P}} - H^{\mathrm{SER}} &= (1-x)^0\, G_{\mathrm{BaO}}^{P} + x^0 G_{\mathrm{Ln2O3}}^{P} \\ &+ RT\,[x \ln x + (1-x)\ln(1-x)] \\ &+ x(1-x)\,\left[\left(a_0 + b_0 T\right) + (1-2x)\left(a_1 + b_1 T\right)\right] \ (\mathrm{Ln} = \mathrm{La, Gd}) \end{aligned} \tag{7}$$

where P represents the solution phase, including liquid, X_{SS}, H_{SS}, A_{SS}, and B_{SS}. ${}^0G_{Ln2O3}{}^P$ and ${}^0G_{BaO}{}^P$ are the Gibbs energy of Ln_2O_3 (Ln = La, Gd) and BaO in P phase, respectively. These values were taken from the literature assessment.[11,20] The interaction parameters a_0, b_0, a_1, and b_1 were to be optimized. Due to the very limited solubility of rare earth oxides in solid BaO,[6] the BaO-based solid solution was treated as the pure oxide.

As illustrated above, the heat capacities of $BaLn_2O_4$ follow the NKR calculation within experimental uncertainty, thus the $BaLa_2O_4$ and $BaGd_2O_4$ compounds were described using the NKR. For the $Ba_3Gd_4O_9$ compound, it was described by the NKR since there were no experimental thermodynamic data in the literature. The Gibbs energies of these compounds were given by the following equations:

$$G_{\mathrm{BaLn2O4}} = G_{\mathrm{BaO}}^{\mathrm{RS}} + G_{\mathrm{Ln2O3}}^{A} + A_1 + B_1 T \ (\mathrm{Ln} = \mathrm{La\ and\ Gd}) \tag{8}$$

$$G_{\mathrm{Ba_3Gd_4O_9}} = 3G_{\mathrm{BaO}}^{\mathrm{RS}} + 2G_{\mathrm{Gd_2O_3}}^{\mathrm{C}} + A_2 + B_2 T \tag{9}$$

where A_i and B_i (i = 1,2) are the parameters related with the enthalpy and entropy of formation from the component oxides.

The PARROT program of the Thermo-Calc software package was used for the parameter optimization. It was started by optimizing the Gibbs energy function of the $BaLn_2O_4$ (Ln = La, Gd) compound. The corresponding values of the measured enthalpy of formation and the assessed entropy of formation based on the second law were used as the starting points during the optimization process. The obtained parameters A and B were then slightly modified when the interaction parameters of the liquid phase were optimized by considering the phase equilibria related to both the $BaLn_2O_4$ compound and liquid phase. For the BaO-La_2O_3 system, the interaction parameters of A_{SS}, H_{SS}, and X_{SS} phases were assessed one by one to fit the corresponding phase equilibria.[6] This work directly used the thermodynamic interaction parameters of the BaO-Sm_2O_3 system as reference to describe the solution phases of the BaO-Gd_2O_3 system, only to optimize the Gibbs energy of formation of $BaGd_2O_4$ and $Ba_3Gd_4O_9$ by considering the thermodynamic data as well as the phase diagram information, including the melting and the decomposition of the compounds.

The final thermodynamic database for the BaO-La_2O_3 and BaO-Gd_2O_3 system is given in Table 3. These parameters

TABLE 3 Summary of the thermodynamic parameters for the BaO–La_2O_3 and BaO–Gd_2O_3 systems according to the present optimization*

$G_{BaO}{}^X = G_{BaO}{}^{RS} + 44\,944$, $G_{BaO}{}^H = G_{BaO}{}^{RS} + 45\,428$
$G_{BaO}{}^A = G_{BaO}{}^{RS} + 54\,914$, $G_{BaO}{}^B = G_{BaO}{}^{RS} + 83\,690$, $G_{BaO}{}^C = G_{BaO}{}^{RS} + 5000$
BaO–La_2O_3 and BaO–Pr_2O_3 systems: Thermodynamic interaction parameters of the solution phases in BaO–La_2O_3 system optimized and listed below and were analogized to calculate the phase diagram of the BaO–Pr_2O_3 system.
liquid phase: $a_0 + b_0T = -94\,086 + 15.4T$, $a_1 + b_1T = 77\,013 - 36.6T$
X_{SS} solution: $a_0 + b_0T = -68\,567 + 0.5T$
H_{SS} solution: $a_0 + b_0T = -41\,210 - 1.43T$
A_{SS} solution: $a_0 + b_0T = -63\,407 - 1.37T$, $a_1 + b_1T = 2861 - 14.7T$
$G(BaLa_2O_4,T) = G_{BaO}{}^{RS} + G_{La2O3}{}^A - 28\,400 + 4.1T$
$G(BaPr_2O_4,T) = G_{BaO}{}^{RS} + G_{Pr2O3}{}^A - 39\,600 + 9T$
BaO–Gd_2O_3, BaO–Eu_2O_3, and BaO–Er_2O_3 systems: Thermodynamic parameters for the solution phases of the above three systems are analogized from the BaO–Sm_2O_3 system
$G_{BaGd2O4} = G_{BaO}{}^{RS} + G_{Gd2O3}{}^B - 56\,500 + 9.7T$
$G_{Ba3Gd4O9} = 3\,G_{BaO}{}^{RS} + 2G_{Gd2O3}{}^C + 69\,256.2 - 83.7T$
$G_{BaEu2O4} = G_{BaO}{}^{RS} + G_{Eu2O3}{}^B - 53\,900 + 8.8T$
$G_{Ba3Eu4O9} = 3\,G_{BaO}{}^{RS} + 2G_{Eu2O3}{}^B + 28\,904 - 61.2T$
$G_{BaEr2O4} = G_{BaO}{}^{RS} + G_{Er2O3}{}^C - 69\,500 + 27T$
$G_{Ba3Er4O9} = 3\,G_{BaO}{}^{RS} + 2G_{Er2O3}{}^C + 106\,308 - 92.8\,T$

*All values are given in SI units (J, mol, K).The Gibbs energy functions of BaO, Ln_2O_3 (Ln = La, Pr, Gd, Eu, Er) can be obtained in literature.[11,20]

together with the Gibbs energies of BaO, La_2O_3, and Gd_2O_3 from the literature[11,20] allow calculations of the thermodynamic properties and the phase diagrams of the BaO-La_2O_3 and BaO-Gd_2O_3 systems.

Comparison between the calculated phase diagram of the BaO–La_2O_3 system with the measured one[6] is shown in Figure 4A. Good agreement is obtained. The calculated BaO–Gd_2O_3 phase diagram is shown in Figure 5A, which displays similar phase relations as those in the BaO–Sm_2O_3 system.[11] Both $BaLa_2O_4$ and $BaGd_2O_4$ are detected to melt in an incongruent process, according to the reactions $BaLa_2O_4 = A_{SS}$ + Liquid and $BaGd_2O_4 = A_{SS} + Ba_3Gd_4O_9$, showing similar behavior to $BaNd_2O_4$ and $BaSm_2O_4$, respectively.[11,12] It should be pointed out that the melting temperatures of the $BaLn_2O_4$ (Ln = La, Nd, Sm, Gd) compounds based on calculations did not show a regular increase from $BaLa_2O_4$ to $BaGd_2O_4$ as reported by Lopato.[6]

6 | DISCUSSION

The enthalpy of formation of $BaGd_2O_4$ from the component oxides determined in this work as well as those

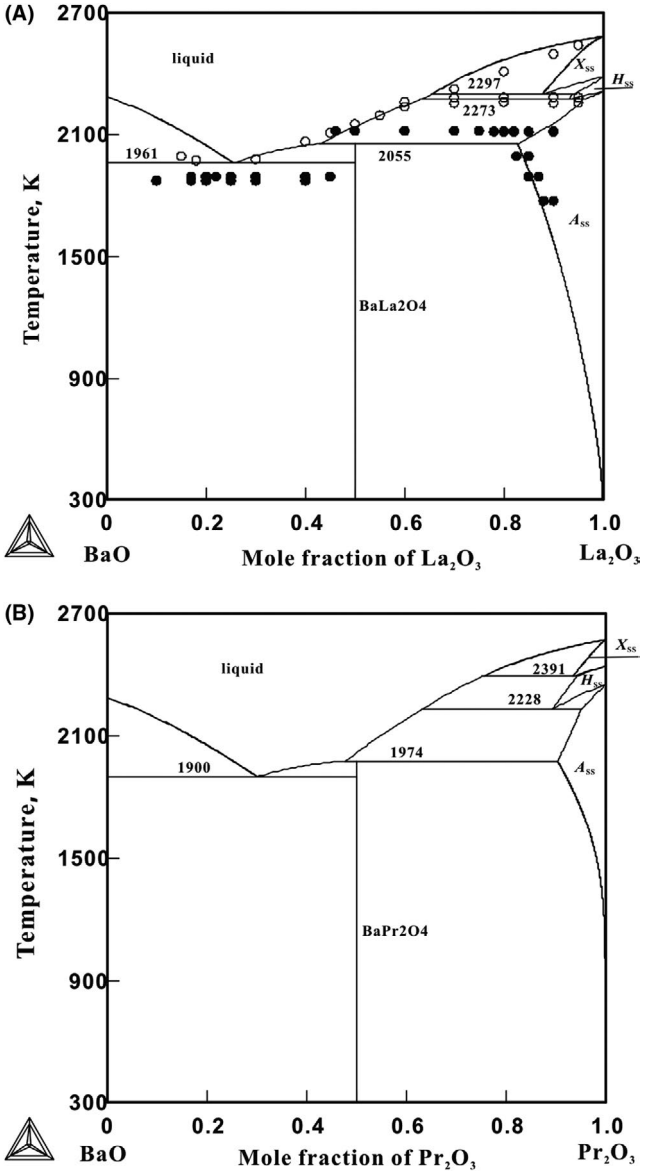

FIGURE 4 A, Calculated BaO-La_2O_3 phase diagram using the thermodynamic parameters optimized in this work. Symbols ● and ○ represent the experimental data obtained by XRD and DTA, respectively.[6] B, Calculated BaO–Pr_2O_3 phase diagram using the thermodynamic parameters analogized from the BaO–La_2O_3 system

of $BaNd_2O_4$ and $BaSm_2O_4$ determined in our previous work[11,12] show that the enthalpies of formation of the $BaLn_2O_4$ compounds become more exothermic in an approximately linear relationship with the increasing radius of the rare earth ion. The heat capacities of $BaGd_2O_4$ measured in this work as well as those of $BaNd_2O_4$ and $BaSm_2O_4$ measured in our previous work[11,12] demonstrate that the $BaLn_2O_4$ compounds fit the NKR calculation in the temperature range measured.

On this basis, the enthalpy of formation and the Gibbs energy of formation of $BaLa_2O_4$ and $BaGd_2O_4$ were evaluated as discussed above. Combined with the phase diagram information in the literature, the phase diagrams of the BaO–La_2O_3 and BaO–Gd_2O_3 systems were calculated, showing similar phase relations as those of the BaO–Nd_2O_3 and BaO–Sm_2O_3 systems, respectively.

As a further test of the thermodynamic model, this work evaluated the Gibbs energy functions of $BaPr_2O_4$, $BaEu_2O_4$, and $BaEr_2O_4$ using the predicted enthalpies of formation based on the relation with the radius of the rare earth ion and the heat capacities calculated by the NKR. The phase diagrams of the BaO–Pr_2O_3, BaO–Eu_2O_3, and BaO–Er_2O_3 systems were calculated using the thermodynamic parameters adapted from assessments of the BaO–La_2O_3 and BaO–Gd_2O_3 systems.

As shown in Figures 4 and 5, the BaO–Pr_2O_3 system has a similar phase diagram as the BaO–La_2O_3 and BaO–Nd_2O_3 systems.[12] The phase diagrams of the BaO–Eu_2O_3 and BaO–Er_2O_3 systems are similar to those of the BaO–Sm_2O_3 and BaO–Gd_2O_3 systems.

The thermodynamic calculations on the BaO–Ln_2O_3 systems indicate that the phase relations of the BaO–Ln_2O_3 systems can be divided into two groups: the first group constitutes the systems from La to Nd, where the $BaLn_2O_4$ compound exists. The second group includes the systems from Sm to Er where there are both $BaLn_2O_4$ and $Ba_3Ln_4O_9$ compounds.

Since the calculated melting temperatures of the $BaLn_2O_4$ (Ln = La, Nd, Sm, Gd) compounds did not show regularity, and no experimental data were reported in the literature, this work detected the melting temperatures of $BaPr_2O_4$, $BaEu_2O_4$, and $BaEr_2O_4$ by thermodynamic calculation. Future high-temperature experiments are required to check the melting temperatures of these compounds.

7 | CONCLUSIONS

Differential scanning calorimetry and high-temperature oxide melt solution calorimetry were used to determine the heat capacity and enthalpy of formation of the $BaGd_2O_4$ compound. The determined heat capacities of the compound are consistent with the NKR calculation. The enthalpy of formation of $BaGd_2O_4$ from component oxides at 298 K is more negative than those of $BaSm_2O_4$ and $BaNd_2O_4$ and shows a linear relationship with the radius of the rare earth ion. Discrepancies between the present determined data and those in the literature are discussed and the reliable experimental data are used to construct the thermodynamic database of the BaO–La_2O_3 and BaO–Gd_2O_3 systems. Thermodynamic calculations support the experimental phase diagram of the BaO–La_2O_3 system in the literature very well and confirm the similar phase relations of the BaO–Gd_2O_3 and BaO–Sm_2O_3 systems. The enthalpies of formation of $BaPr_2O_4$, $BaEu_2O_4$, and $BaEr_2O_4$ and the phase diagrams of the BaO–Pr_2O_3, BaO–Eu_2O_3, and BaO–Er_2O_3 systems are also predicted.

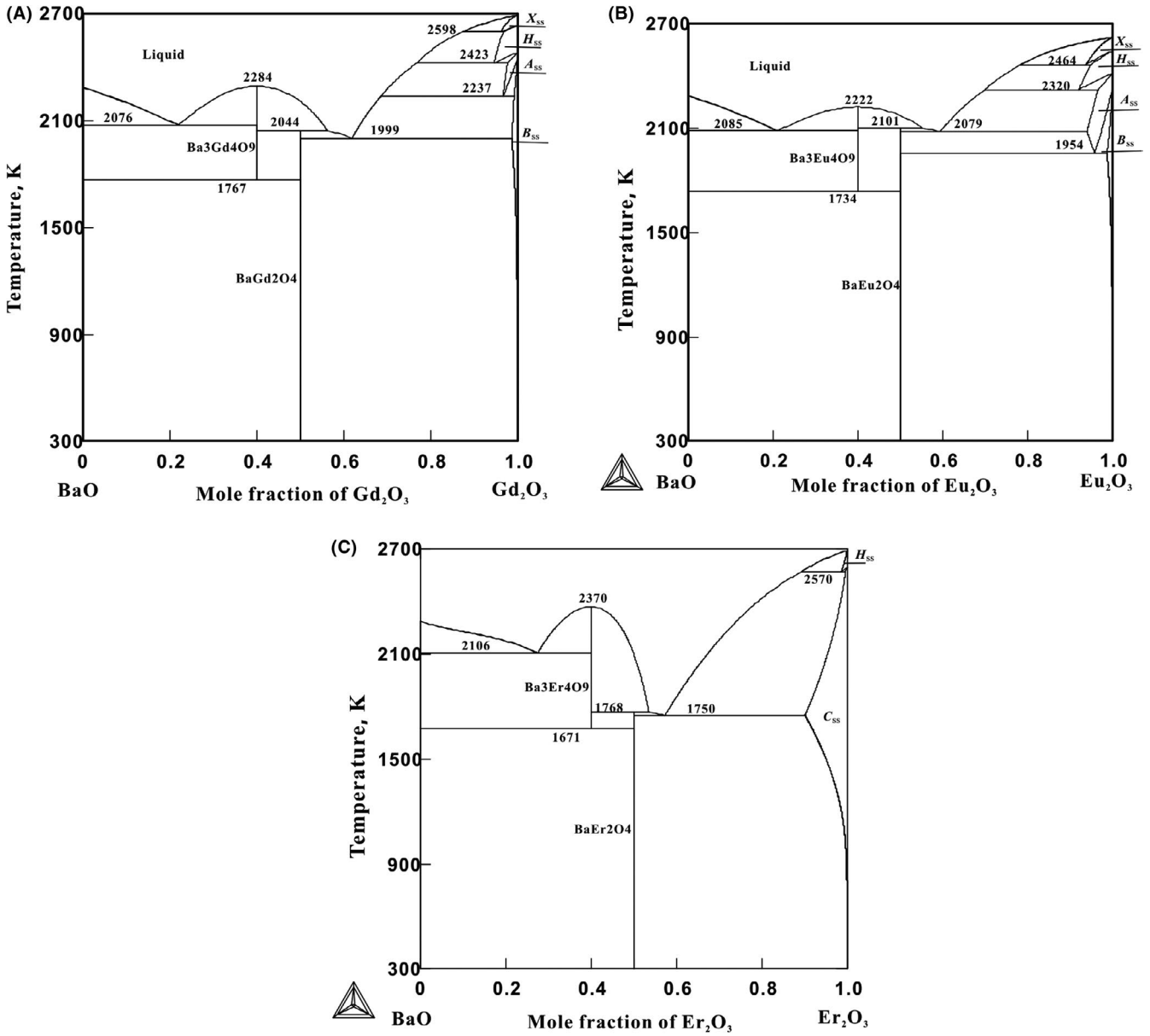

FIGURE 5 A, Calculated BaO–Gd_2O_3 phase diagram using the thermodynamic parameters analogized from the BaO–Sm_2O_3 system. B, Calculated BaO-Eu_2O_3 phase diagram using the thermodynamic parameters analogized from the BaO-Sm_2O_3 system. C, Calculated BaO–Er_2O_3 phase diagram using the thermodynamic parameters analogized from the BaO–Sm_2O_3 system

ACKNOWLEDGMENTS

The funding for Weiping Gong came from the Natural Science Foundation of China (No. 51672100, 51602121, 51171069, 21606053). Support from the National Study Abroad Fund (China), International Science and Technology cooperation project of Guangdong Province (2019A050510049), Natural Science Foundation of Guangdong Province (2017A030310665) as well as the program for Innovative Research Team of Huizhou University (IRTHZU) is greatly appreciated. Experimental work at UC Davis was supported by the US National Science Foundation (grant DMR 1835848).

ORCID

Alexandra Navrotsky https://orcid.org/0000-0002-3260-0364

REFERENCES

1. Kobayashi H, Ogino H, Nakamura K, Mori T, Yamamura H, Mitamura T. Order-disorder transition of BaM_2O_4 (M: La, Nd, Sm, Gd, Ho, Y) bodies synthesized by sintering of $BaCO_3$-M_2O_3 mixtures. J Ceram Soc Jpn. 1994;102:583–6.
2. Doi Y, Nakamori W, Hinatsu Y. Crystal structures and magnetic properties of magnetically frustrated systems $BaLn_2O_4$ and $Ba_3Ln_4O_9$ (Ln = lanthanide). J Phys: Condens Matter. 2006;18:333-344.

3. Besara T, Lundberg MS, Sun JF, Ramirez D, Dong KY, Whalen JB, et al. Single crystal synthesis and magnetism of the $BaLn_2O_4$ family (Ln = lanthanide). Prog Solid State Chem. 2014;42:23–36.
4. Puig T, Martínez B, Yu R, Hu A, Gomis V, Sandiumenge F, et al. Critical currents in air processed $NdBa_2Cu_3O_7$ melt-textured superconductors. Appl Supercond. 1998;6:119–27.
5. Chen IG, Chang FC, Wu MK. Enhancement of the superconducting properties of air-processed melt-growth Sm–Ba–Cu–O with the addition of Sm_2BaO_4. Supercond Sci Technol. 2002;15:717–21.
6. Lopato LM. Highly refractory oxide systems containing oxides of rare-earth elements. Ceram Inter. 1976;2:18–32.
7. Xing XR, Qiao ZY, Wei SK. Thermodynamic properties of complex oxides in the Sm-Ba-Cu-O system. Metall Mater Trans B. 1996;27:973–8.
8. Subasri R, Sreedharan OM. Thermodynamic stabilities of Ln_2BaO_4 (Ln= Nd, Sm, Eu or Gd) by CaF_2-based EMF measurements. J All Comp. 1998;274:153–6.
9. Uspenskaya IA, Vakhovskaya ZS, Efremova MM, Kovba ML, Emelina AL, Dobrokhotova ZV, et al. The thermodynamic properties of Ln_2BaO_4 (Ln = Sm, Dy, Ho). Russ J Phys Chem. 2006;80:529–34.
10. Vakhovskaya ZS, Voskov AL, Kovba ML, Uspenskaya IA. High-temperature thermodynamic properties of Ln_2BaO_4 (Ln = Nd, Gd, Dy, Ho, Er) compounds. J All Comp. 2006;408:257–9.
11. Gong WP, Ushakov SV, Agca C, Navrotsky A. Thermochemistry of $BaSm_2O_4$ and thermodynamic assessment of the $BaO–Sm_2O_3$ system. J Am Ceram Soc. 2018;101:5827–35.
12. Gong WP, Navrotsky A. Thermodynamics of $BaNd_2O_4$ and phase diagram of the $BaO-Nd_2O_3$ system. J Mater Res. 2019;34(19):3337–42.
13. ASTM. Standard Test Method for Determining Specific Heat Capacity by Differential Scanning Calorimetry. Vol ASTM E1269–11. West Conshohocken, PA: ASTM International. 2011.
14. Ditmars DA, Ishihara S, Chang SS, Bernstein G, West ED. Enthalpy and heat-capacity standard reference material: synthetic sapphire (α-Al_2O_3) from 10 to 2250 K. J Res Natl Bur Stand (U S). 1982;87:159–63.
15. Navrotsky A. Progress and new directions in high-temperature calorimetry. Phys Chem Miner. 1977;2:89–104.
16. Navrotsky A. Progress and new directions in high temperature calorimetry revisited. Phys Chem Miner. 1997;24:222–41.
17. Navrotsky A. Progress and new directions in calorimetry: a 2014 perspective. J Am Ceram Soc. 2014;97:3349–59.
18. Zhang Y, Navrotsky A. Thermochemistry of rare-earth aluminate and aluminosilicate glasses. J Non-Cryst Solids. 2004;341:141–51.
19. Levitskii VA. Thermodynamics of double oxides. I. Some aspects of the use of calcium fluoride-type electrolyte for thermodynamic study of compounds based on oxides of alkaline earth metals. J Solid State Chem. 1978;25:9–22.
20. Zinkevich M. Thermodynamics of rare earth sesquioxides. Prog Mater Sci. 2007;52:597–647.
21. Andersson JQ, Helander T, Hoglund L, Shi P, Sundman B. Thermo-calc & dictra, computational tools for materials science. Calphad. 2002;26:273–312.
22. Andersson J-O, Guillermet AF, Gustafson P, Hillert M, Jansson BO, Jönsson BO, et al. A new method of describing lattice stabilities. Calphad. 1987;11:93–8.
23. Redlich O, Kister AT. Algebraic representation of thermodynamic properties and the classification of solutions. Ind Eng Chem. 1948;40:345–9.

How to cite this article: Gong W, Liu Y, Xie Y, Zhao Z, Ushakov SV, Navrotsky A. Thermodynamic assessment of $BaO–Ln_2O_3$ (Ln = La, Pr, Eu, Gd, Er) systems. *J Am Ceram Soc*. 2020;00:1–9. https://doi.org/10.1111/jace.17060